Experimental study on the mechanical behavior of micro fibrillated cellulose reinforced polylactic acid for potential 4D printing applications

Yosef W Adugna [0000-0002-5932-2667], Cristian Medrano Garcia and Hirpa G Lemu[0000-0001-9588-4707]

University of Stavanger, Faculty of Science and Technology, Department of Mechanical and Structural Engineering and Materials Science, Kjell Arholms gate 41, 4021 Stavanger, Norway
yosef.w.adugna@uis.no

Abstract. The integration of polylactic acid (PLA) and micro-fibrillated cellulose (MFC) composites presents potential for sustainable 4D printing, yet challenges remain in balancing mechanical performance and stimuli-responsive functionality. This study investigates PLA-MFC composites (0 – 5 wt% MFC) processed via freeze-drying, ball milling, extrusion, and fused deposition modeling to assess their mechanical behavior and suitability for dynamic applications. Mechanical testing indicated reduction in compressive strength and energy absorption of 54.5% and 59%, respectively, at 5% attributed to MFC fibril agglomeration and inadequate interfacial adhesion, as evidenced by SEM. Flexural modulus also shows competing effects of reinforcement and defect formation. Despite mechanical drawbacks, MFC provided tunable stiffness and moisture sensitivity, critical for 4D-printed structures. Results underscore the necessity of dispersion control, as agglomeration above 2.5% MFC supports brittleness and extrusion inconsistencies. Based on its hygroscopicity, biodegradability, and graded stiffness, this composite can be proposed for applications, for example, in self-actuating packaging, transient medical implants, and adaptive architectural systems. However, achieving reliability demands interfacial optimization via surface treatments or compatibilizers. This work advances eco-conscious 4D printing by demonstrating MFC-PLA's potential to merge environmental responsiveness with moderate structural functionality, contingent on resolving processing challenges.

Keywords: Microfibrillated cellulose, 4D Printing, Fused deposition modelling

1 Introduction

The increasing demand for sustainable materials in additive manufacturing has led to major interest in biopolymers, particularly poly lactic acid (PLA), a renewable and biodegradable thermoplastic sourced from starch-rich crops such as corn and sugarcane [1, 2]. The compatibility of PLA with fused deposition modeling (FDM), its low toxicity, and its moderate mechanical properties establish it as a fundamental material in 3D printing [3, 4]. However, its basic limitations, such as brittleness, low thermal stability, and constrained environmental responsiveness, hinder its utilization in more cutting-edge applications such as 4D printing, where materials are required to dynamically adjust their shape or functionality in reaction to stimuli like heat, moisture, or light [5, 6]. To address these challenges, there has been a growing focus on bio-based reinforcements, with cellulose derivatives standing out as promising options because of their renewability, high stiffness, and ability to improve interfacial bonding [7, 8]. Among them, the capacity of microfibrillated cellulose (MFC) and its micro-scale counterparts to enhance mechanical and thermal properties in polymer composites while maintaining processability has drawn interest [9, 10]. Regardless of these advances, there are still important questions about how MFCs affect PLA composites' shape memory behavior and stimuli-responsive performance, especially when it comes to 4D printing [11, 12].

Although the integration of cellulose reinforcements into PLA matrices has been thoroughly investigated, the majority of research attempts focus on cellulose at the nanoscale (such as nanocrystalline cellulose or cellulose nanofibers) [13, 14]. Although these nanomaterials improve mechanical strength and barrier qualities, their scalability is limited by issues such agglomeration, expensive manufacture, and difficult dispersion techniques [15, 16]. With their larger fibril diameters and lower surface energy, MFC presents a practical substitute that may be able to solve dispersion problems while still being compatible with melt-processing methods such as FDM [17]. However, little is known about how MFCs and PLA interact in 4D printing applications, especially in relation to the effects of fibril size, concentration, and dispersion quality on extrusion consistency and shape memory behavior [18]. Existing studies on PLA-cellulose composites for 4D printing often neglect the balance between enhanced stimuli-responsiveness and mechanical integrity, leaving a critical gap in optimizing these materials for functional applications [8, 19].

The main challenge is achieving MFC-induced thermal responsiveness and shape memory enhancements with PLA composites' mechanical performance. Previous research shows that cellulose concentration beyond 5 wt% can decrease tensile strength and ductility due to poor interfacial adhesion and fibril agglomeration [20]. For 4D printing, where materials undergo repeated shape transitions, such degradation could compromise structural reliability [21]. This study addresses these challenges by experimentally investigating the material behavior of PLA blended with MFCs for FDM-based 4D printing. The objective is to characterize how MFC concentration (0 - 5 wt%) influences the mechanical properties of PLA composite using a combination of freeze-drying, planetary ball milling, extrusion, 3D printing, and mechanical tests (compression and flexural).

2 Materials and methods

2.1 Materials

Microfibrillated cellulose (EXILVA) is collected from Borregaard company, Norway in slurry form for both 2% suspension and 10% paste extracted from Norwegian wood.

While PLA granule is used. The mechanical properties of the materials are listed in Table 1.

Table 1. Parameters of PLA and MFC materials.

	Source	Crystallinity	Melting Temp. (°C)	Tensile strength (MPa)	Elastic modulus (GPa)
PLA	Fermented plant sugars	10 - 40% (semi)	150 -180	50 - 70	2.6 - 3.5
MFC	Plant cellulose	60 – 70%	Degrade at 200	150 - 250	10 - 30

2.2 Material processing and preparation

The MFC is received in slurry form. To ensure the consistent distribution of the cellulose with PLA granule during extrusion, converting into powder is convenient. Freeze-drying (lyophilization) was used to remove the water. Freeze drying consists of three phases, freezing, primary drying, and secondary drying. Exilva F 01-V was divided into 4 trays, containing 125 grams of material, as shown in Figure 1. The material was spread in thin layers (1-3 mm thick) using a spatula to ensure even distribution, allowing for faster and more even drying. The parameters used for freeze-drying is summarized in Table 2.

Fig. 1. Preparation of MFC (a) before (b) during and (c) after freeze-drying

Table 2. MFC freeze-drying parameters.

	Sample (°C)	Condenser (°C)	Vacuum (Pa)	Time (hrs)
Pre-freeze	25 to -36.6	-93.9	101.325	0 - 21
Primary drying	-36.6 to -21.3	-98.8	15	21 - 45
Secondary drying	-21.3 to 24.8	-30.3	101.325	45 - 47

After obtaining the MFC in thin layers, a planetary ball milling machine was used to convert it to fine powder. The MFC and the grinder balls were placed in the grinding bowl maintaining a 5:1 ball-to-powder ratio. The milling parameters were set, with a milling time of 10 minutes and a rest interval of 5 minutes. This cycle was repeated four times, resulting in a total milling time of 60 minutes.

The different types of concentration between the PLA and MFC were determined based on available material quantities and the desired composition for each test specimen as summarized in Table 3. When blending, each component presented a different physical form - PLA in pellets and MFC in powder. To achieve proper dispersion of MFC and avoid the common issue of particle agglomeration, a bioplasticizer Polyethylene glycol 400(PEG 400) was used.

Table 3. Different concentration ratio of PLA-MFC.

Nr.	MFC Concentration %	PLA (wt. in g)	MFC (wt. in g)
1	0	110	0
2	1	594	6
3	2.5	448.7	11.5
4	5	333.25	17.54

2.3 Filament extrusion and 3D printing

The 3Devo filament extruder is used to extrude the MFC-PLA mixture as well as PLA alone to be used as a control. The procedure started by finding the material's melting point, adding mixture to the extruder, and melting them to a molten mass. Table 4 shows the parameters of the extrusion machine.

Table 4. 3Devo extrusion parameters.

Parameters	Values
Filament fan speed	10%
Filament diameter	2.85 mm
Extruding speed	4.2 – 4.4 RPM
Nozzle size	3 mm
Temperature	Feeder zone: 180 ºC Melt zone 1: 183 ºC Melt zone 2: 185 ºC Nozzle: 183 ºC

After the filament was prepared according to the desired concentration, it was fed to the Prusa MK4 FDM printing machine. The file preparation follows slicing the specimens .stl file in Prusaslicer and exporting to the machine using external USB.

Table 5. 3D printing parameters.

Process parameters	Values
Printing temperature	220 ºC
Building plate temperature	60 ºC
Nozzle size	0.3 mm
Nozzle temperature	220 ºC
Temperature 1st layer	215 ºC
Completion rate	100 %
Print orientation	Horizontal
Orientation of layers	45 º

2.4 Mechanical test

The compression test specimen was prepared according to ASTM D695, and the test was performed using INSTRON 5985 test machine having A 10 kN load cell. The test was conducted at a speed of 1.3 ± 0.3 mm/min and was stopped once the specimen reached 30% compressive strain to prevent excessive deformation or flattening of the sample.
Flexural test specimen is also prepared using ASTM D790 and tested on the same machine. A speed of 1 mm/min was used for the test, with 5% strain as the stopping criterion.

2.5 Scanning electron microscopy

The samples were fixed to a platform using adhesives and arranged according to their MFC concentrations. The platform was placed inside a Leica EM SDC 500 for coating the samples with gold, and then imaging completed.

3 Results and Discussion

3.1 Compression test

The compression test data for PLA-MFC composites shows a significant mechanical performance degradation with increasing MFC concentration, highlighting the challenge of using cellulose reinforcements in structural applications as summarized in Table 6. PLA alone has the highest compressive stress (81.18 ± 0.81 MPa) and elastic modulus (277.3 MPa), but these values decrease with MFC incorporation: compressive stress drops by 42.5% at 1% MFC (46.64 ± 0.07 MPa), 51.5% at 2.5% (39.34 ± 3.24 MPa), and 54.5% at 5% (36.93 MPa), while modulus of elasticity drops by 42.5% (159.4 MPa) at 1% and 54.5% (126.3 MPa) at 5% MFC concentration.

Table 6. Compression test data

	Force (kN)	Compressive stress (MPa)	E-module (MPa)
PLA Alone	10.29 ± 0.10	81.18 ± 0.81	277.3
1%	5.91 ± 0.0085	46.64 ± 0.067	159.4
2.5%	4.98 ± 0.41	39.34 ± 3.24	134.5
5%	4.68 ± 0.43	36.93 ± 3.41	126.3

Figure 2 shows the stress-strain curve of different concentrations of MFC-PLA. The steep reductions the compressive strength with the MFC concentration increment suggest poor interfacial adhesion between hydrophilic MFC and hydrophobic PLA, causing agglomeration-induced stress concentrations and failure. The standard deviations are notably high at 2.5% MFC (±3.24 MPa stress vs. ±0.07 MPa at 1%) indicating further signal inconsistent fibril dispersion, likely due to inadequate processing such as solvent incompatibility or insufficient shear mixing.

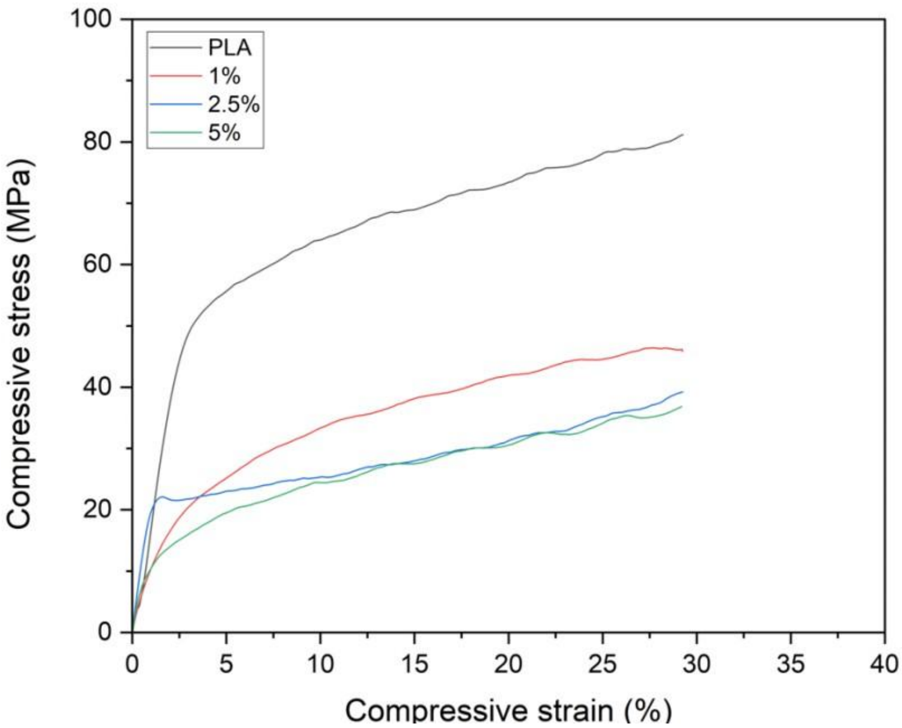

Fig. 2. Stress-strain curve of compression test

The non-linear modulus reduction most declared at 1% MFC suggests the presence of competing mechanisms - limited fibril alignment at low concentrations could limit polymer chain mobility, whereas higher loadings (≥2.5%) can fill the matrix with agglomerates, leading to voids that significantly influence mechanical behavior. This corresponds with flexural data, indicating that the modulus reached its highest point at 1% MFC before declining at 2.5%, implying that the reinforcing potential of MFC is particularly sensitive to dispersion thresholds. For applications, these results caution against using MFC-PLA in load-bearing scenarios but highlight roles where moderate strength is enough, such as biodegradable cushioning or short-term packaging. To salvage potential, future work must prioritize interfacial engineering to enhance stress transfer.

3.2 Results of energy absorption capacity

The energy absorption capacity of PLA-MFC composites shows a significant, concentration-dependent decline (Table 7). PLA alone demonstrates superior energy absorption (62.32 J; SEA 15,580 J/kg), but these values plummet by 46% (33.64 J) at 1% MFC, 56% (27.14 J) at 2.5%, and 59% (25.23 J) at 5% MFC, with specific energy absorption (SEA) mirroring this trend (6,306 J/kg at 5%).

Table 7. Energy absorbed, and specific energy absorbed data.

	Energy Absorbed (J)	**SEA (J/kg)**
PLA Alone	62.32	15580.53
1%	33.64	8402.29
2.5%	27.14	6778.17
5%	25.23	6306.71

Likewise the compression result, and the observed degradation indicate that MFC contributes to the formation of structural defects, such as agglomerates or weak interfacial zones, which facilitate premature fracture and limit plastic deformation and energy dissipation. The poor compatibility of the hydrophilic MFC with hydrophobic PLA contributes to these weaknesses, resulting in stress concentrations that accelerate crack propagation. The non-linear reduction rate indicates a sharp decline at 1% MFC, which gradually narrows at higher loadings. This suggests the presence of a percolation threshold, beyond which additional fibrils contribute minimally to energy absorption losses. This phenomenon may be attributed to the saturation of defect sites or the entanglement of fibrils.

The significant reduction in SEA (59% at 5% MFC) demonstrates an important trade-off: although MFC improves biodegradability, it strongly weakens energy management, posing a risk for impact-resistant applications. The residual SEA of approximately 6,300 J/kg may be adequate for low-energy, transient applications, including biodegradable packaging or agricultural fertilizer films, where moderate energy dissipation corresponds with short-term functional requirements. The fixed strain criterion suggests that all composites demonstrate comparable microscopic ductility in functional applications, though the failure modes may vary significantly. PLA exhibits uniform plastic deformation, whereas MFC composites experience localized cracking, which reduces energy efficiency. This difference limits their effectiveness in dynamic load-bearing applications or impact-resistant structures but is suitable for transient uses where moderate energy absorption and controlled failure are permissible, such as compostable packaging or moisture-activated 4D-printed actuators.

3.3 Flexural test

The flexural test data shows that PLA alone exhibits baseline flexural properties (stress: 57.7 ± 1.12 MPa, modulus: 1434.87 MPa), whereas the MFC incorporation results in non-linear trends. At 1% MFC, the modulus increases by 57% (2255 MPa), indicating partial reinforcement due to restricted polymer chain mobility. Table 8 summarizes the results of flexural strength test.

Table 8. Flexural strength test results

Specimen	Force (kN)	Compressive stress (MPa)	Compressive strain (%)	E-module (MPa)
PLA Alone	0.072 ± 0.001	57.7 ± 1.12	4.023 ± 0.208	1434.87
1%	0.057 ± 0.005	47.057 ± 5.46	2.087 ± 0.046	2255.48
2.5%	0.0367 ± 0.011	31.157 ± 8.67	3.973 ± 0.392	784.08
5%	0.052 ± 0.009	41.82 ± 6.87	2.263 ± 0.241	1847.80

However, stress decreases by 18% (47.06 MPa) and strain reduces by 48% (2.087%), which suggests embrittlement. This paradox indicates that MFC fibrils at low concentrations may increase stiffness while also introducing stress-concentrating defects. At 2.5% MFC, significant degradation is observed that modulus decreases by 45% (784 MPa), stress declines by 46% (31.16 MPa), and strain variability increases (±0.392%), indicating severe agglomeration or interfacial failure. The partial recovery observed at 5% MFC (modulus: 1848 MPa, stress: 41.82 MPa) suggests the presence of fibril networking or alignment, however, the properties are still inferior to those of PLA alone.

The strain-modulus mismatch indicates that a higher strain of 3.973% occurs at 2.5% MFC, despite a lower stiffness. This suggests potential changes in failure modes, such as microcracking versus ductile flow. The variability in modulus (2255 MPa at 1% versus 784 MPa at 2.5%) may facilitate graded stiffness in 4D-printed structures; however, strength reductions may hinder reliability. To enhance MFC's potential, interfacial engineering, such as silane treatments, and advanced processing techniques, including solvent-assisted dispersion, are essential for reducing agglomeration. These composites may be appropriate for transient, low-stress applications (e.g., humidity-responsive actuators) where adjustable stiffness is prioritized over mechanical shortcomings.

3.4 Scanning electron microscopy

The SEM image of PLA containing 2.5% MFC (Figure 3) shows notable fiber pull-out and interfacial debonding, as indicated in the marked area. In contrast to pure PLA, which displayed a more organized layered morphology characterized by voids and openings between the layers, the incorporation of MFC results in more intricate fracture patterns. The presence of MFC fibers indicates an effort to improve mechanical reinforcement; however, the observable fiber pull-out signifies inadequate interfacial adhesion between PLA and MFC. The weak bonding might reduce the anticipated enhancements in strength and toughness, resulting in localized stress concentrations and premature failure. The rougher and more porous fracture surface in PLA-MFC, in contrast to the smoother and more brittle fractures of pure PLA, indicates enhanced energy absorption during fracture. The presence of voids and debonding indicates potential processing challenges, including inadequate dispersion and insufficient interfacial compatibility. Enhancing the performance of PLA-MFC composites may involve implementing improved fiber-matrix adhesion strategies, including chemical surface modifications or compatibilizers, to reduce fiber pull-out and strengthen mechanical properties.

The incorporation of elevated concentrations of MFC into PLA matrices may induce agglomeration, leading to clustering and the formation of voids within the composite. Defects in FDM processes are significant, as uneven fiber distribution interferes with layer deposition, resulting in inadequate interlayer adhesion and increased voids. Inconsistencies can compromise the mechanical integrity of printed components, as voids and inadequate layer adhesion can serve as stress concentrators, thereby diminishing the overall strength and durability of the final product. To address these issues, optimizing the dispersion of MFC within the PLA matrix is crucial, potentially through surface treatments or the application of compatibilizers, to achieve uniform distribution and improve interfacial bonding. Moreover, precise regulation of FDM processing parameters, including extrusion temperature and printing speed, can reduce defect formation and enhance the quality of printed composites.

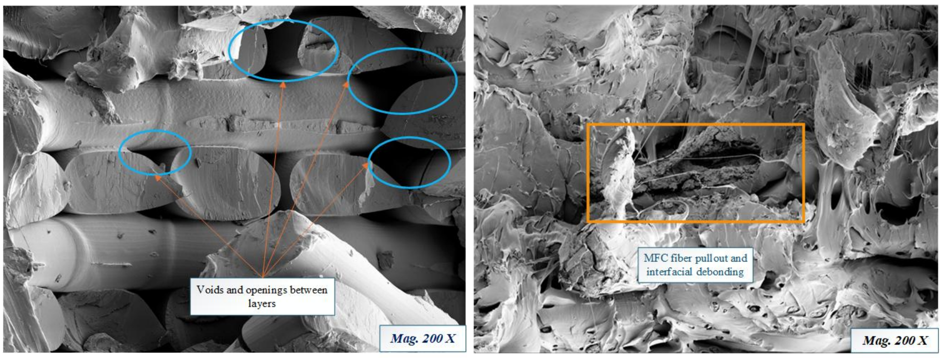

PLA alone PLA – 2.5%MFC

Fig. 3. SEM of PLA alone and PLA-MFC

The strain-modulus mismatch indicates that a higher strain of 3.973% occurs at 2.5% MFC, despite a lower stiffness. This suggests potential alterations in failure modes, such as microcracking versus ductile flow, which cannot be verified without fractography. The observed non-monotonic modulus trend contradicts established filler-composite theory, prompting inquiries into interfacial bonding and testing alignment. In the absence of standardized parameters, such as the span-to-depth ratio, the reproducibility of results remains questionable.

The variability in modulus (2255 MPa at 1% versus 784 MPa at 2.5%) may facilitate graded stiffness in 4D-printed structures; however, strength reductions and data dispersion hinder reliability. To enhance MFC's potential, interfacial engineering, such as silane treatments, and advanced processing techniques, including solvent-assisted dispersion, are essential to reduce agglomeration. These composites may be appropriate for transient, low-stress applications (e.g., humidity-responsive actuators) where adjustable stiffness is prioritized over mechanical shortcomings, provided that stringent quality control and microstructural validation are implemented.

4 Conclusion and future outlooks

The mechanical behavior of PLA- MFC composites indicated declining strength and energy absorption, but tunable stiffness and moisture-sensitive properties make them appealing for advanced applications. MFC reduces compressive strength (54% loss at 5% MFC), flexural modulus (non-linear variability), and energy absorption (59% SEA decline at 5% MFC), but these compromises align with emerging domains where sustainability, stimuli-responsiveness, and graded functionality dominate over mechanical performance. Critically, MFC's hygroscopicity and PLA's biodegradability offer unique 4D printing and transient, eco-conscious prospects, particularly in the following areas of biodegradable shape-morphing packaging, medical implants/devices with programmable degradation, sustainable soft robotics and wearables and adaptive architectural membranes

The moisture-triggered deformability of MFC-PLA, due to its hygroscopic fibrils, could enable self-folding packaging that responds to environmental humidity, decreasing logistics waste, Example can be flat-packed containers that self-assemble when wet during transport. Low compressive strength (36.93 MPa at 5% MFC vs. 81.18 MPa for PLA) is sufficient for lightweight, short-term packaging, and biodegradability meets circular economy requirements. The utilization of modulus variability (e.g., 2255 MPa at 1% MFC for rigidity vs. 784 MPa at 2.5% for flexibility) to create multilayer implants that soften during tissue healing. Lower energy absorption (~6307 J/kg at 5% MFC) could prevent stress shielding in bone scaffolds. MFC’s biocompatibility and PLA’s resorbability make these composites suitable for temporary stents or sutures that degrade after fulfilling their function.

The partial modulus recovery at 5% MFC (1848 MPa) and moisture-triggered strain (2.263% strain at 5% MFC) could enable soft actuators for agricultural or marine robotics that use water/moisture as an activation stimulus. The moderate SEA (~6307 J/kg) enables energy dissipation during repetitive motions (e.g., grippers, sensors), while biodegradability reduces environmental impact if devices are misplaced or abandoned. The use of graded MFC concentrations in 4D-printed structures could produce building skins that adjust to humidity, enhancing shading and ventilation. The flexural modulus reduction at 2.5% MFC (~784 MPa) may allow for hinge-like zones for reversible shape modifications. To realize these applications, interfacial engineering is required to reduce agglomeration-induced deficiencies. Hybrid systems using shape-memory PLA or dynamic covalent networks may improve recyclability and multi-stimuli responsiveness even though lifecycle assessments and standardized environmental testing (humidity, temperature) are necessary to prove feasibility.

References

1. Hegab, H., et al., *Design for sustainable additive manufacturing: A review.* Sustainable Materials and Technologies, 2023. **35**: p. e00576.
2. Taib, N.-A.A.B., et al., *A review on poly lactic acid (PLA) as a biodegradable polymer.* Polymer Bulletin, 2023. **80**(2): p. 1179-1213.
3. Tümer, E.H. and H.Y. Erbil, *Extrusion-based 3D printing applications of PLA composites: a review.* Coatings, 2021. **11**(4): p. 390.
4. Ramot, Y., et al., *Biocompatibility and safety of PLA and its copolymers.* Advanced drug delivery reviews, 2016. **107**: p. 153-162.
5. Farah, S., D.G. Anderson, and R. Langer, *Physical and mechanical properties of PLA, and their functions in widespread applications—A comprehensive review.* Advanced drug delivery reviews, 2016. **107**: p. 367-392.
6. Vashishtha, G., et al., *Shaping the future: latest developments in 3D printing stimuli-responsive soft polymers.* The International Journal of Advanced Manufacturing Technology, 2025: p. 1-23.
7. Shaghaleh, H., X. Xu, and S. Wang, *Current progress in production of biopolymeric materials based on cellulose, cellulose nanofibers, and cellulose derivatives.* RSC advances, 2018. **8**(2): p. 825-842.
8. Gauss, C., K.L. Pickering, and L.P. Muthe, *The use of cellulose in bio-derived formulations for 3D/4D printing: A review.* Composites Part C: Open Access, 2021. **4**: p. 100113.
9. Youssef, A.M. and S.M. El-Sayed, *Bionanocomposites materials for food packaging applications: Concepts and future outlook.* Carbohydrate polymers, 2018. **193**: p. 19-27.
10. Jakob, M., et al., *The strength and stiffness of oriented wood and cellulose-fibre materials: A review.* Progress in Materials Science, 2022. **125**: p. 100916.
11. Sajab, M.S., et al., *Nanocellulose-based composites for 3D printed stimuli-responsive swelling hydrogel.* Industrial Crops and Products, 2024. **222**: p. 119541.
12. Khalid, M.Y., et al., *Shape-memory and self-healing properties of sustainable cellulosic nanofibers-based hybrid materials for novel applications.* Giant, 2024: p. 100299.
13. Abdulkhani, A., et al., *Preparation and characterization of modified cellulose nanofibers reinforced polylactic acid nanocomposite.* Polymer testing, 2014. **35**: p. 73-79.
14. Eichhorn, S.J., et al., *Current international research into cellulose as a functional nanomaterial for advanced applications.* Journal of Materials Science, 2022. **57**(10): p. 5697-5767.
15. Mariano, M., N. El Kissi, and A. Dufresne, *Cellulose nanocrystals and related nanocomposites: Review of some properties and challenges.* Journal of Polymer Science Part B: Polymer Physics, 2014. **52**(12): p. 791-806.
16. Jakubek, Z.J., et al., *Characterization challenges for a cellulose nanocrystal reference material: dispersion and particle size distributions.* Journal of Nanoparticle Research, 2018. **20**: p. 1-16.
17. Khalil, H.A., et al., *A review on micro-to nanocellulose biopolymer scaffold forming for tissue engineering applications.* Polymers, 2020. **12**(9): p. 2043.

18. Muthuraj, R., M. Misra, and A.K. Mohanty, *Biodegradable compatibilized polymer blends for packaging applications: A literature review.* Journal of Applied Polymer Science, 2018. **135**(24): p. 45726.
19. Muthe, L.P., K. Pickering, and C. Gauss, *A review of 3D/4D printing of poly-lactic acid composites with bio-derived reinforcements.* Composites Part C: Open Access, 2022. **8**: p. 100271.
20. Lee, C.H., A. Khalina, and S.H. Lee, *Importance of interfacial adhesion condition on characterization of plant-fiber-reinforced polymer composites: A review.* Polymers, 2021. **13**(3): p. 438.
21. Zhang, Z., B. Cao, and N. Jiang, *The mechanical properties and degradation behavior of 3D-printed cellulose nanofiber/polylactic acid composites.* Materials, 2023. **16**(18): p.6197.